Modelling of coupled multifield problems in concrete by means of porous media mechanics

F. Pesavento & B. A. Schrefler
Dept. of Structural and Transportation Engineering, University of Padova, Padova, Italy

D. Gawin
Dept. of Building Physics and Building Materials, Technical University of Lodz, Lodz, Poland

ABSTRACT: A mathematical and numerical model to predict the non-linear behaviour of concrete as a multiphase porous material is proposed. The model can be usefully applied to several practical cases: evaluation of concrete performance in the high temperature range, e.g. during fire, to early stages of maturing of massive concrete structures, to shotcrete in tunnelling, and to durability processes (e.g. leaching/carbonation). All the important phase changes of water and chemical reactions, i.e. adsorption-desorption, condensation-evaporation, and hydration-dehydration, skeleton dissolution/carbonation as well as the related heat and mass sources or sinks are considered. Changes of the material properties caused by temperature and pressure changes, concrete damage, carbonation, leaching, fresh concrete hardening, as well as coupling between thermal, hygral, chemical and mechanical phenomena are taken into account. This model further allows to incorporate sorption hysteresis. Some relevant applications of the model will be shown in this work.

1 INTRODUCTION

In several situations it is necessary to model concrete as a multiphase material, i.e. a material made up of a solid phase and pores which are filled with water (capillary and physically adsorbed), vapour and dry air. Typical cases deal with concrete performance in the high temperature range, e.g. during fire, with early stages of maturing of massive concrete structures with shotcrete in tunnelling, and with durability.

We present here a general model for chemo-hygro-thermo-mechanical analysis of concrete applicable to the above situations using a mechanistic approach.

Such a kind of approach leads to governing equations that are usually more complicated formally, but their coefficients have clear physical meaning and often are related to classical material parameters, like for example porosity, intrinsic permeability, diffusivity of vapour in air, etc. When some relations between structure parameters and transport properties are found (e.g. effect of water degree of saturation on relative permeability for water flow), usually they are valid for a class of similar materials, e.g. cellular concrete, ceramic materials, etc. Often models of this group are obtained from microscopic balance equations written for particular constituents of the medium, which are then averaged in space, e.g. by means of Volume Averaging Technique, mixture theory or homogenisation theory. Mass and energy fluxes are usually expressed by means of gradients of the related thermodynamic potentials, e.g. temperature, capillary pressure, water vapour concentration etc. Phase changes and the related mass- and energy sources (sinks) are usually taken into account. Moreover, some additional couplings, e.g. effect of material damaging on intrinsic permeability or capillary and vapour pressures (moisture content) on skeleton stresses, can be considered.

In this paper the model mentioned above is applied to the case of concrete at early ages and beyond and to the case of concrete structures under fire.

2 PHYSICAL AND MATHEMATICAL MODEL

Moist concrete is modelled as a multi-phase material, which is assumed to be in thermo-dynamic equilibrium state locally. The voids of the skeleton are filled partly with liquid water and partly with a gas phase. The liquid phase consists of bound water, which is present in the whole range of moisture content, and capillary water, which appears when water content exceeds the upper limit of the hygroscopic region, S_{ssp}. The gas phase is a mixture of dry air and water vapour, and is assumed to be an ideal gas. The chosen primary variables of the model are: gas pressure p^g, capillary pressure $p^c = p^g - p^w$ (p^w denotes water pressure), temperature T, displacement vector of the solid matrix $\mathbf{u}$, and finally carbon dioxide concentration ρ_d if carbonation process is considered, while the internal variables are: degree of cement hydration Γ_{hydr}, when hydration or dehydration phe-

nomena are analysed, degree of carbonation Γ_{carb}, when carbonation is taken into account and mechanical damage d and thermo-chemical damage V when damaging-deterioration processes are considered. Hence, the general mathematical model of chemo-hygro-thermo-mechanical processes consists of four or five balance equations, depending on the problem analysed. They are completed by an appropriate set of constitutive and state equations, and some thermodynamic relationships. Considering that in this work we do not take into account the case of concrete subjected to carbonation phenomenon (durability mechanics) and that in the case of concrete structures exposed to high temperatures in the range below 600-700°C we can neglect the term related to decarbonation process, the final form of the set of governing equations is:

- *Mass balance equation of the dry air:*

$$-n\frac{D^s S_w}{Dt} - \beta_s\left(1-n\right)S_g\frac{D^s T}{Dt} + S_g \, div\,\mathbf{v}^s + \frac{S_g n}{\rho^{ga}}\frac{D^s \rho^{ga}}{Dt}$$
$$+\frac{1}{\rho^{ga}}div\,\mathbf{J}_g^{ga} + \frac{1}{\rho^{ga}}div\left(n S_g \rho^{ga}\mathbf{v}^{gs}\right)+ \qquad (1)$$
$$-\frac{\left(1-n\right)S_g}{\rho^s}\frac{\partial\rho^s}{\partial\Gamma_{hydr}}\frac{D^s\Gamma_{hydr}}{Dt} = \frac{\dot{m}_{hydr}}{\rho^s}S_g$$

- *Mass balance equation of the water species:*

$$n\left(\rho^w - \rho^{gw}\right)\frac{D^s S_w}{Dt} + \left(\rho^w S_w + \rho^{gw}S_g\right)\alpha\,div\,\mathbf{v}^s +$$
$$+div\,\mathbf{J}_g^{gw} + div\left(n S_w\rho^w\mathbf{v}^{ws}\right)+div\left(n S_g\rho^{gw}\mathbf{v}^{gs}\right)+$$
$$-\left(\rho^w S_w + \rho^{gw}S_g\right)\frac{\left(1-n\right)}{\rho^s}\frac{\partial\rho^s}{\partial\Gamma_{hydr}}\frac{D^s\Gamma_{hydr}}{Dt} + S_g n\frac{D^s\rho^{gw}}{Dt} = \qquad (2)$$
$$= \frac{\dot{m}_{hydr}}{\rho^s}\left(\rho^w S_w + \rho^{gw}S_g - \rho^s\right)$$

- *Enthalpy balance equation of the multi-phase medium:*

$$\left(\rho C_p\right)_{eff}\frac{\partial T}{\partial t} + \left(\rho_w C_p^w\mathbf{v}^w + \rho_g C_p^g\mathbf{v}^g\right)\cdot grad\,T +$$
$$-div\left(\lambda_{eff}\,grad\,T\right) = -\dot{m}_{vap}\Delta H_{vap} + \dot{m}_{dehydr}\Delta H_{dehydr} \qquad (3)$$

- *Linear momentum conservation equation of the multi-phase medium:*

$$div\left(\boldsymbol{\sigma}_e^s - \alpha\,p^s\,\mathbf{I}\right)+\rho\mathbf{g} = 0 \qquad (4)$$

where the effective stresses $\boldsymbol{\sigma}_e^s$ is given by:

$$\boldsymbol{\sigma}_e^s = (1-D)\boldsymbol{\Lambda_0} : \left(\boldsymbol{\varepsilon}_{tot} - \boldsymbol{\varepsilon}_{th} - \boldsymbol{\varepsilon}_0\right) \qquad (5)$$

where the parameter D is the total damage resulting from various material deterioration processes of different nature: mechanical, thermo-chemical, purely chemical.

The term $\boldsymbol{\varepsilon}_0$ in eq. (5) is formed by two different contributions: chemical strains accounting for thermo-chemical deterioration process in case of elevated temperatures or chemical reactions in all the other cases, and creep strains accounting for mid-long term creep in durability problems and thermal creep in high temperature ranges:

$$\boldsymbol{\varepsilon}_0 = \boldsymbol{\varepsilon}_{chem} + \boldsymbol{\varepsilon}_{creep} \qquad (6)$$

The mass balance equation of carbon dioxide has to be added to the previous ones if carbonation phenomenon is analysed. Furthermore, three (or more) evolution equations, corresponding to the internal variables related to the evolution processes included in the model, can be added to the above described governing equations:

- *Hydration/Dehydration process evolution law:*
When dehydration process is considered (temperature higher than 105°C), taking into account its irreversibility, one may assume that the degree of dehydration depends on the maximum value of temperature reached during heating:

$$\Gamma_{dehydr}\left(t\right) = \Gamma_{dehydr}\left(T_{max}\left(t\right)\right) \qquad (7)$$

while, when hydration process is analyzed (below 105°C) the hydration degree is defined in the following way:

$$\Gamma_{hydr} = \frac{\chi}{\chi_\infty} = \frac{m_{hydr}}{m_{hydr\infty}} \qquad (8)$$

where m_{hydr} means mass of hydrated water (chemically combined), χ is the hydration extent and χ_∞, $m_{hydr\infty}$ are the final values of hydration extent and mass of hydrated water, respectively.

- *Thermo-chemical damage evolution equation (high temperature):*
The parameter V takes into account both effects of concrete dehydration (chemical component) and material cracking (mechanical component) on material degradation and the Young's modulus decrease with increasing temperature. It is obtained from the experimental results, and is a function of the maximum temperature reached during heating because of the irreversible character of the material structural changes:

$$V\left(t\right) = V\left(T_{max}\left(t\right)\right) \qquad (9)$$

- *Mechanical damage evolution equation:*
The mechanical damage parameter d is expressed in terms of the equivalent strain, $\tilde{\varepsilon}$, and it is given by equations of the classical non-local, isotropic damage theory,

$$d\left(t\right) = d\left(\tilde{\varepsilon}\left(t\right)\right) \qquad (10)$$

Similarly to what has been stated for governing equations, if carbonation process is taken into account in the modelling of concrete behaviour, it is necessary to define the corresponding evolution

equation. For a full description of the model and its mathematical formulation, see Pesavento (2000) and Gawin et al. (2003, 2004, 2006a,b).

3 EFFECTIVE STRESS IN CONCRETE

Due to the porous multi-phase nature of concrete, after application of an external load the material deforms not only due to this load, but also due to the pressure exerted on the skeleton by fluids present in its voids. The physical nature of the interaction between particles of water and concrete skeleton on micro-structural level is rather complex. This interaction depends mainly on the pore dimensions and moisture content and is caused by joint effects of capillary tension, disjoining pressure and surface tension of solids (Bazant 1988), Figure 1. It results in macroscopic deformations of concrete structures. These phenomena can be described by means of the effective stress. A more complete expression defining it for materials with fine pores and well developed internal structure, where surface adsorption phenomena are of importance, like for example in concrete, has been recently obtained in (Gray & Schrefler 2001) by exploitation of entropy inequality for porous media partially saturated with water.

The total stress $\boldsymbol{\sigma}$ may be split into the effective stress $\boldsymbol{\sigma}_e^s$, which accounts for stress effects due to changes in porosity, spatial variation of porosity and the deformations of the solid matrix, and the solid pressure p^s, (Gray & Schrefler 2001),

$$\boldsymbol{\sigma} = \boldsymbol{\sigma}_e^s - \alpha p^s \mathbf{I}, \tag{11}$$

where p^s is the solid phase pressure exerted by the pore fluids (liquid water and moist air), $\boldsymbol{\sigma}$ the total stress tensor, $\mathbf{I}$ the unit tensor of second order, and

$$\alpha = 1 - K_T / K_s \tag{12}$$

is the Biot coefficient accounting for different values of bulk moduli for solid phase (grain) and the skeleton, K_s and K_T. In eq.(11) stresses are positive in traction and fluid pressures are positive in compression.

At low levels of saturation, water is present in pores primarily as a thin film on the skeleton surface. Some of the liquid water – gas interfaces have curvatures influenced by the skeleton shape and the solid phase equilibrium pressure is defined by:

$$p^s = \chi_s^{ws} \left(p^w + s^{ws} J_{ws}^s \right) + \left(1 - \chi_s^{ws} \right) \left(p^g + s^{gs} J_{gs}^s \right), \tag{13}$$

where χ_s^{ws} is the fraction of skeleton area in contact with water, J_{ws}^s, J_{gs}^s the average curvatures of the solid-water and solid-gas phase interfaces, respectively, s^{ws}, s^{gs} are interfacial tension like terms, $p^w = p_o^w - \Pi^f$ is the water film pressure, with Π^f the water film disjoining pressure and p_o^w the reservoir water pressure. The equilibrium capillary pressure can be written as:

$$p^c \equiv p^g - p^w = \Pi^f - s^{wg} J_{wg}^w \tag{14}$$

where s^{wg} is water surface tension and J_{wg}^w the average curvature of the water-gas phase interface.

Thus the pressure difference between the fluid phases is due to curvature of the interface and the disjoining pressure, which is important for thin films. At moderate levels of water saturation, when capillary forces dominate and the adsorbed water film effects are of less importance, the disjoining pressure in eqs. (13) and (14) may be neglected. Rearranging eq.(13) and applying eq.(14), we obtain,

$$\begin{aligned} p^s &= p^g + \chi_s^{ws} s^{wg} J_{wg}^w - \chi_s^{ws} \Pi^f \\ &+ \chi_s^{ws} s^{ws} J_{ws}^s + \left(1 - \chi_s^{ws} \right) s^{gs} J_{gs}^s, \end{aligned} \tag{15}$$

where one can recognize terms corresponding to the main physical phenomena mentioned in (Bazant 1988) as causes of concrete shrinkage. The first term on the R.H.S. describes an effect of gas pressure (it is negligible), the second one of capillary tension, the third one of disjoining pressure, and the last two terms, resulting from action of surface tension of solids on the interfaces with the pore fluids, can be neglected. Due to a very complex micro-structure of concrete, it is practically impossible to apply eq. (15) in this form. Instead, a simplified relationship, based on the measurable value of capillary pressure, (14), taking also into account disjoining pressure, can be used, Gray &Schrefler (2001), Gawin et al. (2004),

$$\boldsymbol{\sigma}_e^s = \boldsymbol{\sigma} + \alpha \left(p^g - \chi_s^{ws} p^c \right) \mathbf{I}, \tag{16}$$

where the material function $\alpha \chi_s^{ws} \left(S_w \right)$ and saturation degree of pores with liquid water $S_w(p^c)$ (i.e. the so called sorption isotherms) should be determined experimentally at ambient of various relative humidities corresponding to vapour-liquid thermodynamic equilibrium of water in pores of different sizes.
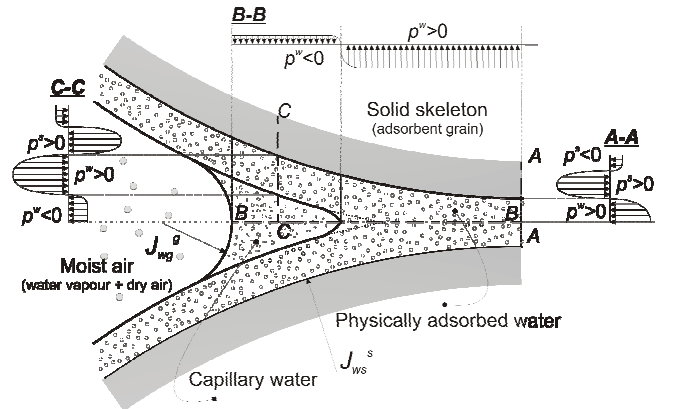

Figure 1: Idealized sketch of the adsorbed layer of water with transition to the macro-pore, pressures in water and in a skeleton.

4 MODELING OF HYDRATION PROCESS

From the macroscopic point of view, hydration of cement is a complex interactive system of competing chemical reactions of various kinetics and amplitudes. They are associated with complex physical and chemical phenomena at the micro-level of material structure, (de Schutter & Taerwe 1995, de Schutter 2002), resulting in considerable changes of macroscopic concrete properties. Kinetics of cement hydration (hydration rate) cannot be described properly in terms of equivalent age nor maturity of concrete, if the effect of the reaction rate on temperature (and/or relative humidity) depends upon the hydration degree, or chemical affinity of the reaction is affected by temperature variations (and/or relative humidity) (Jensen & Hansen 1999). Hence, another thermodynamically based approach has been used instead, similarly as proposed by Ulm and Coussy (1995, 1996), see Gawin et al. (2006a,b). In this approach the hydration extent χ is the advancement of the hydration reaction and its rate is related to the affinity of the chemical reaction through an Arrhenius-type relationship, as usual for thermally activated chemical reactions, Gawin et al. (2006a,b):

$$\frac{d\chi}{dt} = \tilde{A}_\chi(\chi)\exp\left(-\frac{E_a}{RT}\right) \tag{17}$$

where $\tilde{A}_\chi(\chi)$ is normalized affinity (it accounts both for chemical non-equilibrium and for the nonlinear diffusion process), E_a – hydration activation energy, and R – universal gas constant. Equation (17) can be rewritten in terms of hydration degree, defined as in eq. (8), and relative humidity by means of a function $\beta\varphi(\varphi)$, (φ is the relative humidity), Gawin et al. (2006a,b):

$$\frac{d\Gamma_{hydr}}{dt} = \tilde{A}_\Gamma\left(\Gamma_{hydr}\right)\beta_\varphi(\varphi)\exp\left(-\frac{E_a}{RT}\right) \tag{18}$$

An analytical formula for the description of the normalized affinity of the following form,

$$\tilde{A}_\Gamma\left(\Gamma_{hydr}\right) = A_1\left(\frac{A_2}{\kappa_\infty} + \kappa_\infty \Gamma_{hydr}\right)\left(1 - \Gamma_{hydr}\right)\exp\left(-\bar{\eta}\,\Gamma_{hydr}\right) \tag{19}$$

was proposed by Cervera et al. (1999) and is used in our model. The coefficients A_1, A_2 and $\bar{\eta}$ can be obtained from the temperature evolution during adiabatic tests.

5 MODELLING OF CONCRETE CREEP

Creep is modelled here by means of the solidification theory (Bazant 1988, Bazant & Prasannan 1989) for the description of the basic creep, and micro-prestress theory (Bazant et al. 1997a,b) for the description of the long-term creep and the stress induced creep (part of the so called drying creep). Thus, according to the solidification theory proposed by Bazant and Prasannan (1989) aging is considered as the result of a solidification process involving basic constituents, which do not have aging properties. Due to cement hydration, new products, in particular calcium silicate hydrates (C-S-H), can precipitate forming new layers of material able to sustain an external load (these layers at the beginning are stress-free). The load-bearing components of concrete exhibit both viscous flow and visco-elastic deformation. The increase of global stiffness of the system is the result of a progressive growth of solidified material fraction. In this manner it is possible to formulate non-aging constitutive laws for these basic constituents, considering a certain micro-compliance function $\Phi(t,t')$ (or alternatively a relaxation function) which can be expanded in Dirichlet series, while all the effects related to aging are described by the solidification process. The definition of micro-compliance or micro-relaxation functions for solidifying material, allows to overcome some well known ill-posed problems associated to the Dirichlet series expansion of global compliance (or relaxation) function formulated for the general behaviour of the material (aging visco-elasticity), see Bazant & Prasannan (1989). In view of this theory the total creep strain increment, $d\varepsilon_c$, is decomposed in two components, the visco-elastic, and the viscous flow strain increments, $d\varepsilon_v$ and $d\varepsilon_f$:

$$d\varepsilon_c = d\varepsilon_v + d\varepsilon_f \tag{20}$$

with $\quad d\varepsilon_v = \frac{F(\sigma_e^s)}{\Gamma_{hydr}}d\gamma$, $\quad d\varepsilon_f = \frac{F(\sigma_e^s)}{\eta}\mathbf{G}\sigma_e^s dt \tag{21}$

where γ is the visco-elastic micro-strain, i.e. the strain of C-S-H gel whose volume fraction grows in time, and a matrix $\mathbf{G}$ is defined in such a way that $\varepsilon = E^{-1}\mathbf{G}\sigma$, where σ and ε are stress and strain vectors, respectively, Gawin et al. (2006b). The apparent macroscopic viscosity, η, is not constant in time and is defined by means of microprestress theory (Bazant et al. 1997a),

$$\frac{1}{\eta(S)} = cpS^{p-1} , \tag{22}$$

where S is the microprestress, while c and p are material constants defined positive. In the current model concrete is treated as a multiphase porous medium, so the stresses in eq.s (21) should be interpreted as the effective ones, σ_e^s, and not the total ones, σ, as in the original theory of Bazant and Prasannan (1989) and Bazant et al. (1997a,b). In such a way it is possible to couple the free shrinkage with the creep, obtaining creep strains even if the concrete structure is externally unloaded. The capilary forces (15) represent, in fact, an "internal" load for the microstructure of the material skeleton. It should be underlined that the non-dimensional solidified fraction function $v(t)$, introduced by Bazant

and Prasannan (1989), in the solidification theory is identified with the hydration degree Γ_{hydr} in eq. (21). The function $F\left(\sigma_e^s\right)$ accounts for the effects of micro-cracking, i.e. non-linear dependence of creep on the stresses (in the case of high stress levels). Similarly to Bazant et al. (1997a,b) it is possible to define the creep compliance function as follows:

$$J(t,t') = q_1' + \Phi(t,t') + cpS^{p-1},\qquad(23)$$

where $\Phi(t,t')$ is visco-elastic micro-compliance function related to the growth of hydration products fraction and defined by eq. (8), the third term on the RHS derives directly from the microprestress theory, and q_1' is the term related to elastic strains:

$$q_1' = \frac{1}{E(\Gamma_{hydr})}.\qquad(24)$$

As proved by Bazant et al. (1997a), the micro-compliance function $\Phi(t,t')$ can be expanded in Dirichlet series which correspond to a Kelvin chain formed by N non aging units, i.e. units whose parameters are constant like in classical visco-elasticity and rheological models. It results in a consistent model from a thermodynamic point of view, i.e. it is possible to avoid strange situations in which the chain spring modulus E_μ results negative in certain time intervals. In the model of concrete creep presented here we have assumed that the microprestresses evolution and the related component of creep strains are influenced by the macro-stresses. If an opposite assumption is made, as suggested in Bazant et al (1997a), the Pickett's effect cannot be modelled properly, as shown by extensive numerical tests described in Gawin et al. (2006a). Hence, it may be assumed that application of the external load acts as a kind of triggering mechanism which activates the flow creep. Physically this could be explained by breakage of atomic bonds at the creep sites at micro-structural level due to a rapid change of the concrete stress state and resulting perturbation in their local force equilibrium, that initiates further shear slips in cement gel. These manifest themselves at the macro-level as creep strains. The latter assumption applied in the current model of concrete strains allows for proper modelling of the Pickett's effect when the effective stresses are used for determination of the creep strains, Bryant & Vadhanavikkit (1987). It should also be underlined that in the current creep model there are no parameters dependent on the concrete relative humidity which were used in the original model of Bazant et al. (1997a,b).

6 MODELLING OF HIGH TEMPERATURE EFFECTS

The model has been applied to the analysis of behaviour of concrete structures under severe temperatures and pressures.

In these conditions concrete structures experience spalling phenomenon, which results in rapid loss of the surface layers of the concrete at temperature exceeding about 200-300°C. As a result, the core concrete is exposed to these temperatures, thereby increasing the rate of heat transmission to the core part of the element and in particular to the reinforcement, what may pose a risk for the integrity of concrete structure. It is commonly believed that the main reasons of the thermal spalling are: build-up of high pore pressure close to the heated concrete surface as a result of rapid evaporation of moisture, and the release of the stored energy due to the thermal stresses resulting from high values of restrained strains caused by temperature gradients. Nevertheless, relative importance of the two factors is not established yet and still needs further studies, both experimental and theoretical. The results of the research performed up to now show, that the fire performance of concrete structures is influenced by several factors, like initial moisture content of the concrete, the rate of temperature increase (fire intensity), porosity (density) and permeability of the concrete, its compressive strength, type of aggregate, dimensions and shape of a structure, its lateral reinforcement and loading conditions. The HSC structures are particularly affected by this phenomenon. In fact, HSC provides better structural performance, especially in terms of strength and durability, compared to traditional, normal-strength concrete (NSC). However, many studies, showed that the fire performance of HSC differs from that of NSC which exhibits rather good behaviour in these conditions. An unloaded sample of plain concrete or cement stone, exposed for the first time to heating, exhibits considerable changes of its chemical composition, inner structure of porosity and changes of sample dimensions. The concrete strains during first heating, called load-free thermal strains (LFTS), (Khoury 1995), are usually treated as superposition of thermal and shrinkage components, and often are considered as almost inseparable. LFTS are decomposed in three main contributions, Gawin et al. (2004):

- *Thermal dilatation strains,*

$$d\boldsymbol{\varepsilon}_{th} = \beta_s(T)\,dT\qquad(25)$$

- *Capillary shrinkage strains,*

$$d\boldsymbol{\varepsilon}_{sh} = \frac{\alpha}{K_T}\left(dx_s^{ws}\,p^c + x_s^{ws}\,dp^c\right)\mathbf{I}\qquad(26)$$

- *Thermo-chemical strains*

$$d\boldsymbol{\varepsilon}_{tchem} = \beta_{tchem}(V)\,dV\qquad(27)$$

Where $\beta_{tchem}(V)$ is obtained from experimental tests. As far as the first contribution is concerned, the strains are treated in a manner usual in thermo-mechanics, but considering the thermal expansion

coefficient β_s as a function of temperature. Shrinkage strains are modelled by means of the effective stress principle in the form derived in section 3. In heated concrete, above the temperature of about 105°C, the thermal decomposition of the cement matrix takes place, and at higher temperatures also that of aggregate (depending on its type and composition). This is a consequence of several complicated, endothermic chemical reactions, called concrete dehydration. As their result a considerable shrinkage of cement matrix (called chemical shrinkage) and usually expansion of aggregate are observed. Due to these contradictory behaviour of the material components, cracks of various dimensions are developing when temperature increases, causing an additional change of concrete strains (usually expansion). These strains are modelled as function of thermo-chemical damage which takes into account the thermo-chemical deterioration of the material. Also the so called LITS, (Khoury 1995), has been considered in the computation. During first heating, mechanically loaded concrete exhibits greater strains as compared to the load-free material at the same temperature. These additional deformations are referred to as load induced thermal strains (LITS), (Khoury 1995, Gawin et al. 2004). A part of them originates just from the elastic deformation due to mechanical load, and it increases during heating because of thermo-chemical and mechanical degradation of the material strength properties. The time dependent part of the strains during transient thermal processes due to temperature changes, is generally called thermal creep. The formulation employed into the model is due to Thelandersson (1987) in its original form, here modified using a coefficient $\bar{\beta}_{tr}(V)$ as a function of thermo-chemical damage V (and not constant) and the effective stresses instead of total stresses, coupling in this way the thermo-chemo-mechanical damage model and capillary shrinkage model with thermal creep model:

$$d\varepsilon_{tr} = \frac{\bar{\beta}_{tr}(V)}{f_c(T_a)} \mathbf{Q} : \tilde{\sigma} \, dV \tag{28}$$

where $\mathbf{Q}$ is a fourth order tensor, $\tilde{\sigma}$ is the effective (in the sense of damage mechanics) stress tensor and finally f_c is the compressive strength of the material at 20°C. The model in this form can be successfully applied to several real cases. For further details see Pesavento (2000), Gawin et. al (2003, 2004).

7 NUMERICAL EXAMPLES

7.1 *Model application to concrete at early ages and beyond*

This numerical example is part of a comprehensive validation of our model of concrete, treated as multiphase porous medium, using published results of the experimental study, (Bryant & Vadhanavikkit 1987), performed for analysing the long-term behaviour of concrete. It concerns the strains of concrete specimens (slabs with thickness of 30 cm), both in sealed and drying conditions, without any external load and loaded at different ages. The initial values of microprestress for the cases with loads applied at different age of concrete were assumed similarly as in Bazant et al. (1997a). We studied the cases when the load (7 MPa) was applied after t=8, 28, 84 and 182 days after the concrete set. For all the cases convective boundary conditions for heat exchange with α_c= 5 W/m²K were assumed, and for the drying specimens convective mass exchange with β_c= 0.002 m/s. The comparison of our simulations results with the experimental data for the strains of the drying specimens (i.e. the shrinkage and drying creep strains) is presented in Figure 2. These results show a really good agreement, even with the characteristic shape of the curves, both for concrete at early ages and after several months from its set. The results obtained for the tests of shrinkage (drying + external load), basic creep (sealed specimen + load) and drying creep (drying + load), (Fig. 2B), show that the Pickett's effect is modelled properly what confirms our assumption about evolution of the creep strains related to microprestresses. For a more detailed description of the model validation, see Gawin et al. (2006a,b).
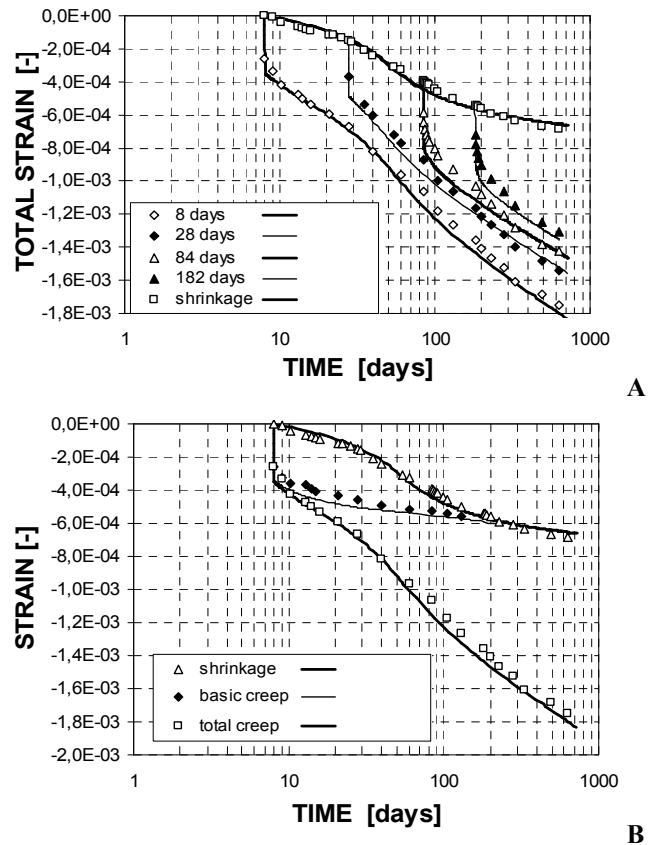

A

B

Figure 2. Comparison of the simulations results with the experimental results, A) drying specimen loaded at different ages (total creep), B) concrete strains in two drying slabs: unloaded (shrinkage), loaded at age t=8 days (total creep), and the sealed, loaded (t=8 days) slab (basic creep).

7.2 Model application to the case of heated concrete

This example deals with a comparison between numerical results, obtained using the model described in the previous sections, and experimental results, obtained from compressive tests carried out in United States in the laboratories of NIST (i.e. National Institute of Standard and Technology) (Phan 1996, Phan et al. 2001, Phan & Carino 2002). The main goal of this comparison is to show the capability of the code to assess spalling phenomena, in particular occurrence of explosive spalling in concrete structures subjected to elevated temperatures. The specimens, cylinders with diameter of 100 mm and height of 200 mm, have been tested using three test methods, representing the thermo-mechanical loading conditions: stressed test method (specimens were preloaded, with a load equal to 40% of final compressive strength at room temperature, and then heated), unstressed test method (specimens were directly heated until the time of compressive test), residual property test method (the specimens were heated up to the target temperature and kept at this temperature for a certain period; then they were cooled and tested at room temperature, i.e. at residual conditions). Five target temperatures, 100°C, 200°C, 300°C, 450°C and 600°C were reached during the tests by means of furnace heating rate of 5°C/min, in steady state conditions. In this case "steady state" is defined as the temperature state when the temperature at the centre of the specimen is within 10°C of the pre-selected target temperature T and the difference between the surface and centre temperatures of the concrete specimen is less than 10°C. Our attention was focused on specimens made of concrete type 1, herein indicated as MIX1 in unstressed conditions with a target temperature equal to 450°C. In fact, for unstressed tests, explosive spalling occurred in all MIX1 specimens heated to 450°C. Initial and boundary conditions used in numerical simulation are listed in Gawin et al. (2004). Figure 3A shows the temperature differences between the surface and the centre of the specimens measured during the tests and the corresponding numerical results. The accordance between numerical and experimental results is quite good. The first part of heating shows a strange behaviour with temperature difference between core and surface practically zero for more than one hour. Figure. 3D provides information about damaging of the specimen during heating. Specifically, it shows the history of total damage in three different points (on the surface, in the centre and in the middle of the radius). The evolution of creep strain is shown in Figure 3C for three different points. Figure 3B shows developments (in three points) of the gas pressure versus temperature compared to the water vapour pressure developments in saturated conditions (red line). The time range between 120 and 150 min seems to be the
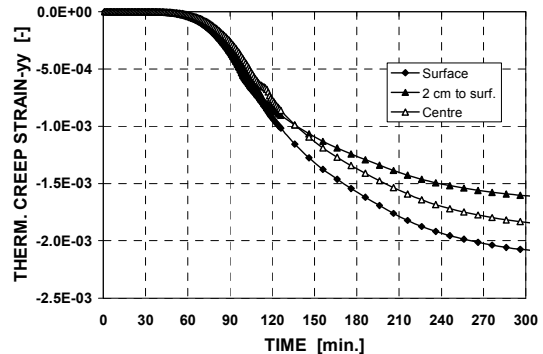
critical range during which the material achieves a state favourable to spalling occurrence; the specimen experienced explosive spalling right in this range of time.
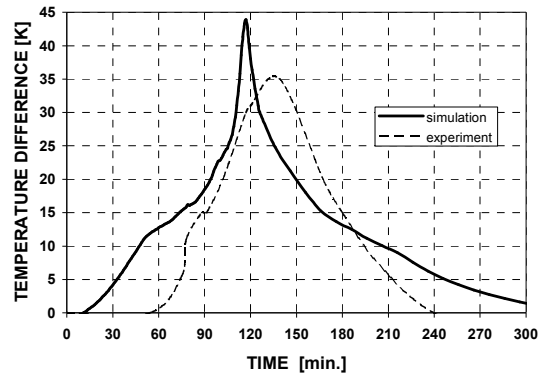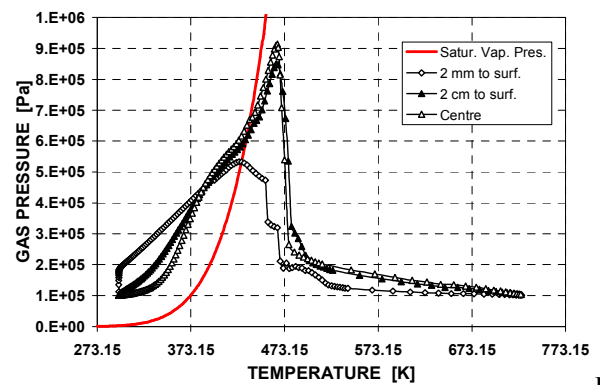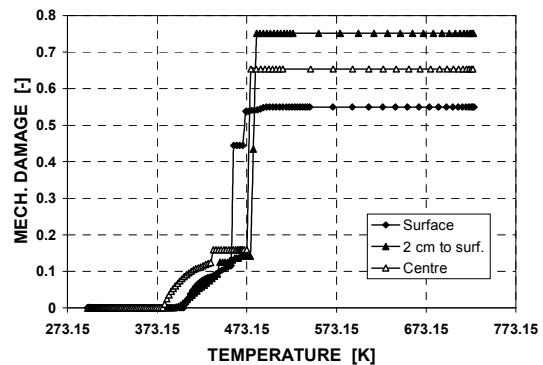

Figure 3: Cylindrical specimen exposed to high temperature: A) Temperature differences history in the specimen (and comparison with experimental results), B) Gas pressure versus temperature in three different points and saturated vapour pressure (red line), C) Creep strains history according to eq. (19), D) Mechanical damage versus temperature in three different points.

Corresponding to the maximum value of ΔT, a sharp increase of mechanical damage parameter d (with a maximum value equal to 80%) may be observed. Similarly to the increase of mechanical damage, the peak of gas pressure corresponds to the maximum value of temperature differences ΔT. The presented results of numerical simulations, show that both pore pressure and thermally induced strains can be identified as responsible for the spalling occurrence, and that they play a primary or secondary role depending on the particular conditions prevailing. For the analysed HPC concretes, the MIX 1 specimens, having lower value of the w/c ratio, spalled explosively mainly due to the high gas pressure value and relatively high level of thermo-chemical deterioration.

8 CONCLUSIONS

A general model for the non-linear modelling of concrete behaviour has been presented in this work. All relevant mass and heat transport phenomena, chemical reactions, phase changes as well as their mechanical effects are taken into account. The richness of the model allows for its application to several practical cases such as the analysis of hydration and aging processes in massive concrete structures and the analysis of the response of concrete structures exposed to high temperatures. The results obtained are in good agreement with the experimental data. The current model can be considered a predictive one for the above mentioned conditions.

REFERENCES

Bazant, Z.P. & Prasannan, S. 1989. Solidification theory for concrete creep. I: Formulation. *Journal of Engineering Mechanics ASCE* 115: 1691-1703.

Bazant, Z.P. 1988. *Mathematical Modelling of Creep and Shrinkage of Concrete*. Chichester: John Wiley & Sons Ltd.

Bazant, Z.P., Hauggaard, A.B., & Baweja, S. 1997b. Microprestress-solidification theory for concrete creep. II: Algorithm and verification, *Journal of Engineering Mechanics ASCE* 123(11): 1195-1201.

Bazant, Z.P., Hauggaard, A.B., Baweja, S. & Ulm, F.J. 1997a. Microprestress-solidification theory for concrete creep. I: Aging and drying effects. *Journal of Engineering Mechanics ASCE* 123(11): 1188-1194.

Bryant, A.H. & Vadhanavikkit C. 1987. Creep, shrinkage-size, and age at loading effects. *ACI Materials Journal.* March-April: 117-123.

Cervera, M., Olivier, J. & Prato T. 1999. A thermo-chemo-mechanical model for concrete I: Hy-dration and aging. *ASCE J. Eng. Mech* 125(9): 1018-1027.

de Schutter, G. & Taerwe, L. 1995. General hydration model for Portland cement and blast furnace slag cement. *Cement Concrete Res.* 25(3): 593-604.

de Schutter, G. 2002. Influence of hydration reaction on engineering properties of hardening con-crete. *Mater. Struct.* 35: 453-461.

Gawin, D., Pesavento, F. & Schrefler, B.A. 2003. Modelling of hygro-thermal behaviour of concrete at high temperature with thermo-chemical and mechanical material degradation. *Comp. Meth. Appl. Mech. Engrg.* 192: 1731-1771.

Gawin, D., Pesavento, F. & Schrefler, B.A. 2004. Modelling of deformations of high strength concrete at elevated temperatures. *Materials and Structures* 37(268): 218-236.

Gawin, D., Pesavento, F. & Schrefler, B.A. 2006a. Hygro-thermo-chemo-mechanical modelling of concrete at early ages and beyond. Part I: Hydration and hygro-thermal phenomena. *Int. J. Num. Meth. Engng* 67: 299–331.

Gawin, D., Pesavento, F. & Schrefler, B.A. 2006b. Hygro-thermo-chemo-mechanical modelling of concrete at early ages and beyond. Part II: Shrinkage and creep of concrete. *Int. J. Num. Meth. Engng* 67: 332-363.

Gray, W.G. & Schrefler, B.A. 2001. Thermodynamic Approach to Effective Stress in Partially Saturated Porous Media. *European Journal of Mechanics A/Solids* 20: 521-538.

Jensen, O.M. & Hansen, P.F. 1999. Influence of temperature on autogenous deformation and relative humidity change in hardening cement paste. *Cem. Concr. Res.* 29: 567-575.

Khoury, G.A. 1995. Strain components of nuclear-reactor-type concretes during first heating cy-cle. *Nuclear Engng and Design* 156: 313-321.

Pesavento, F. 2000. Non-linear modelling of concrete as multi-phase porous material in high temperature conditions. Ph.D. thesis, Padova: University of Padova.

Phan, L.T. & Carino, N.J. 2002. Effects of test conditions and mixture proportions on behavior of high-strength concrete exposed to high temperature, *ACI Materials Journal* 99(1): 54-66.

Phan, L.T. 1996. Fire performance of high-strength concrete: a report of the state-of-the-art. *Research Report NISTIR 5934*, Gaitherburg : National Institute of Standards and Technology.

Phan, L.T., Lawson, J.R. & Davis F.L. 2001. Effects of elevated temperature exposure on heating char-acteristics, spalling, and residual properties of high performance concrete. *Materials and Structures* 34: 83-91.

Thelandersson, S. 1987. Modeling of combined thermal and mechanical action on concrete. *J. Engng Mech. ASCE* 113(6): 893-906.

Ulm F.-J., & Coussy, O. 1995. Modeling of thermo-chemo-mechanical couplings of concrete at early ages. *J. Eng. Mech. ASCE* 121(7): 785-794.

Ulm, F.-J. & Coussy, O. 1996. Strength growth as chemo-plastic hardening in early age concrete. *J. Eng. Mech. ASCE* 122(12): 1123-1132.